RSC Advances

PAPER

View Article Online
View Journal | View Issue

Cite this: *RSC Adv.*, 2023, **13**, 14361

A simple method for the synthesis of copper nanoparticles from metastable intermediates†

Ruihan Lu,[a] Wuchang Hao,[b] Long Kong,[a] Keliang Zhao,[c] Hao Bai[c] and Zhenguo Liu *[ac]

Copper nanoparticles have attracted a wide attention because of their low cost and high specific surface area. At present, the synthesis of copper nanoparticles has the problems of complicated process and environmentally unfriendly materials like hydrazine hydrate and sodium hypophosphite that would pollute water, harm human health and may even cause cancer. In this paper, a simple and low-cost two-step synthesis method was used to prepare highly stable and well-dispersed spherical copper nanoparticles in solution with a particle size of about 34 nm. The prepared spherical copper nanoparticles were kept in solution for one month without precipitation. Using non-toxic L-ascorbic acid as the reducing and secondary coating agent, polyvinylpyrrolidone (PVP) as the primary coating agent, and NaOH as the pH modulator, the metastable intermediate CuCl was prepared. Due to the characteristics of the metastable state, copper nanoparticles were rapidly prepared. Moreover, to improve the dispersibility and antioxidant, the PVP and L-ascorbic acid were used to coat the surface of copper nanoparticles. Finally, the mechanism of the two-step synthesis of copper nanoparticles was discussed. This mechanism mainly relies on the two-step dehydrogenation of L-ascorbic acid to obtain copper nanoparticles.

Received 17th February 2023
Accepted 4th April 2023

DOI: 10.1039/d3ra01082a

rsc.li/rsc-advances

1. Introduction

Compared with conventional metallic materials, metallic nanomaterials have received great attention due to their unique chemical and physical properties.[1] When the material size reaches the nanometer scale, its optical, thermal, and electromagnetic properties undergo an abrupt change, resulting in small size, surface, and quantum size effects.[2–5] Therefore, nanomaterials could be used in several areas such as biosensors, catalysts, adsorbents, and electronic devices.[6–8] Among these metallic nanomaterials, copper nanoparticles have gradually attracted the attention of researchers for their great advantages in cost and specific surface area. The current methods for synthesizing copper nanoparticles are mainly divided into physical and chemical methods. Physical methods include mechanical ball milling, physical vapor deposition, and gas evaporation, while the chemical methods include liquid-phase chemical reduction, chemical deposition, electrochemical method, and hydrothermal method.[9–12] In these methods, the liquid-phase chemical reduction method is widely used because of the controllable particle size and simple process compared with the high equipment cost and uncontrollable process of the physical method. R. Y. Li and *et al.* produced copper nanoparticles with copper sulfate as copper source, potassium borohydride as reducing agent, and polyvinylpyrrolidone (PVP) and cetyltrimethylammonium bromide (CTAB) as dispersants, respectively. The average particle size was 20 nm.[13] W. K. Han and *et al.* prepared copper nanoparticles with a particle size of 100 nm in sodium chloride solution with CuO nanoparticles as the anode and Pt as the cathode. The obtained copper nanoparticles were well distributed without agglomeration.[14] N. Sarwar and *et al.* synthesized copper nanoparticles with a particle size of 120 nm using sodium hypophosphite as reducing agent and citric acid as dispersant.[15] However, it is still a challenge to synthesize copper particles with good dispersion using more environmentally friendly materials.

In recent years, green chemistry has been gradually advocated as society pays more attention to environmental protection.[16,17] The advent of green chemistry requires the use of non-toxic substances and the production of non-toxic substances. In response to the requirements, many scientists have carried out green synthesis of copper nanoparticles, and the key to these syntheses is non-toxic chemicals and environmentally friendly solvents.[18–21] Therefore, in this paper, we report a novel method

[a]*Printing Electronics Center for Flexible Electronics and Institute of Flexible Electronics (IFE), Northwestern Polytechnical University, 1 Dongxiang Road, Xi'an, 710129, China. E-mail: iamzgliu@nwpu.edu.cn*

[b]*Xi'an Hongxing Electronic Paste Technology Co., Ltd, 1099 Dingkunchi 3rd Road, Xi'an, 710199, China*

[c]*Flexible Electronics Center, Ningbo Institute of Northwestern Polytechnical University, 218 Qingyi Road, Ningbo, 315048, China*

† Electronic supplementary information (ESI) available. See DOI: https://doi.org/10.1039/d3ra01082a

for the preparation of copper nanoparticles using anhydrous copper chloride as the copper source, ethylene glycol as the solvent, L-ascorbic acid as the reducing agent, and PVP as the dispersant. The method adopts the liquid-phase chemical reduction method with a two-step reduction mechanism utilizing two-step dehydrogenation of L-ascorbic acid. The copper source was firstly reduced to the metastable intermediate CuCl, and then rapidly reduced to copper nanoparticles. Furthermore, by relying on the reaction between PVP and L-ascorbic acid, the dehydrogenation product of L-ascorbic acid can coat on the surface of copper nanoparticles, it can improve the dispersibility and antioxidant by supplemental coating where PVP fails to cover. The process is simple and green, the prepared copper nanoparticles are well dispersed, and the copper nanoparticle solution does not precipitate for one month.

2. Experimental

2.1 Materials

Anhydrous copper chloride ($CuCl_2$, Sinopharm) was used as a precursor for the preparation of copper nanoparticles. L-Ascorbic acid (Sinopharm) was used as a reducing agent. PVP was used as a dispersant and coating agent. Ethylene glycol (EG, Sinopharm) and deionized water were used as solvents. Sodium hydroxide (NaOH, Sinopharm) was used as a pH modulator.

2.2 Preparation of copper nanoparticles

The preparation of copper nanoparticles includes anhydrous copper chloride, ethylene glycol, L-ascorbic acid, PVP, deionized water, and sodium hydroxide. The entire experiment process was divided into two steps.

2.2.1 Step 1. Firstly, a certain amount of ethylene glycol, anhydrous copper chloride and PVP were weighed. The ethylene glycol was added to beaker A, and then the PVP and anhydrous copper chloride were added to beaker A in order. The molar concentration of Cu^{2+} is 0.37 M, and the amount of PVP added is one-fourth of anhydrous copper chloride. A certain amount of L-ascorbic acid and deionized water were weighed to prepare the L-ascorbic acid solution of 0.5 M. The beaker A was heated to 70 °C and stirred for 30 min, then the prepared L-ascorbic acid solution was added to beaker A and stirred for 10 min. After dropping to room temperature, the intermediate product was

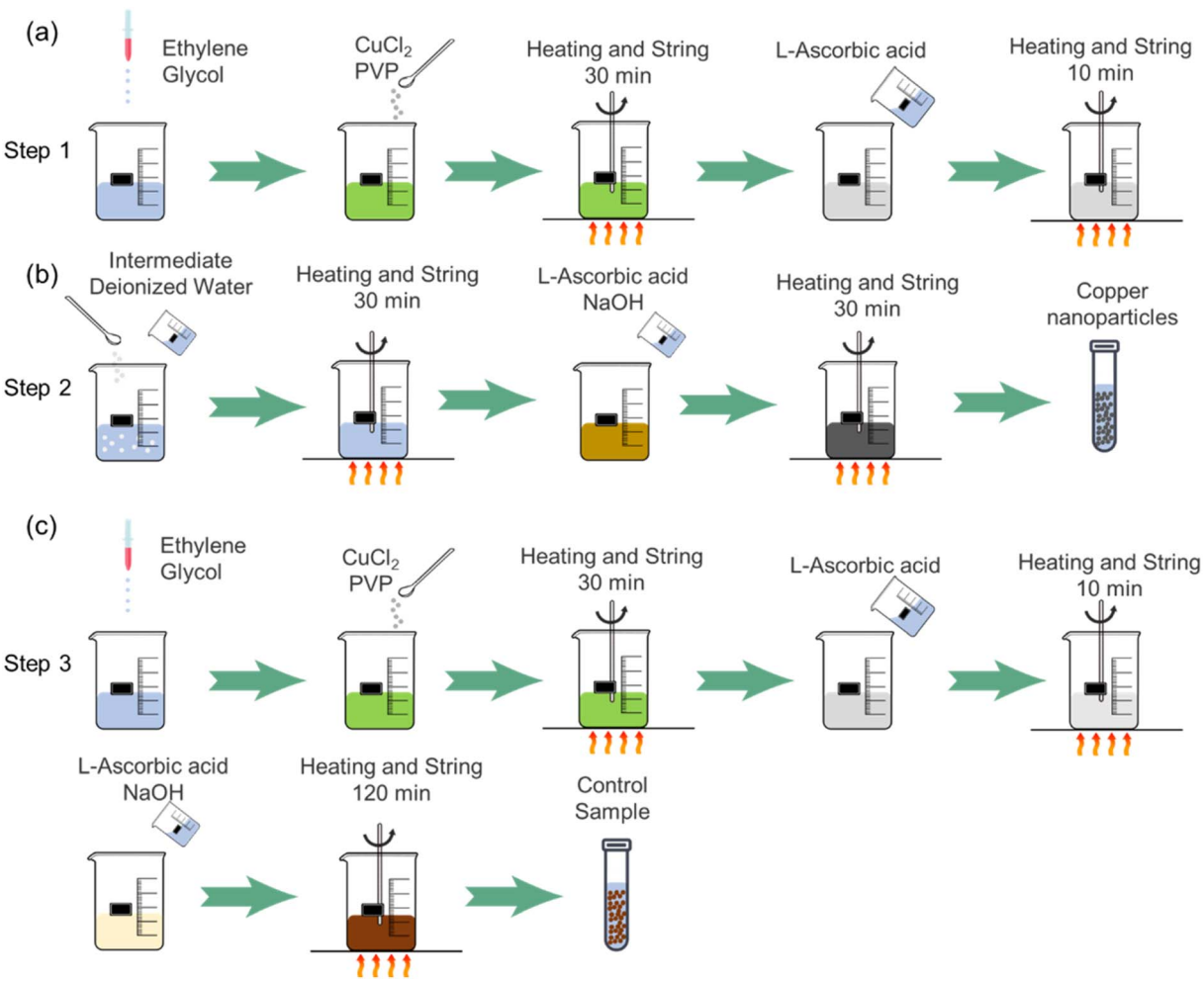

Fig. 1 Schematic diagram of copper nanoparticle synthesis method of (a) Step 1; (b) Step 2 and (c) Step 3.

obtained by centrifuging, washing and vacuum drying. The process is shown in Fig. 1(a).

2.2.2 Step 2. The dried intermediate product and 10 ml of deionized water were added to beaker B. Then 0.5 M NaOH solution and 0.5 M L-ascorbic acid solution using deionized water as solvent were prepared. The beaker B was then heated to 70 °C and stirred for 30 min, then the NaOH and L-ascorbic acid solutions were poured into beaker B and stirred for 30 min. After dropping to room temperature, the copper nanoparticles were obtained by centrifuging, washing and vacuum drying. The process is shown in Fig. 1(b).

As a comparison, a control group was designed based on Step 3.

2.2.3 Step 3. Firstly, a certain amount of ethylene glycol, anhydrous copper chloride and PVP were weighed. The ethylene glycol, PVP and anhydrous copper chloride were added sequentially to beaker C with a 0.37 M Cu^{2+}, and the amount of PVP added is one-fourth of anhydrous copper chloride. While beaker C was heated to 70 °C and stirred for 30 min, the 0.5 M of L-ascorbic acid solution was prepared with deionized water. When the above process was completed, adding the prepared L-ascorbic acid solution to beaker C and stirring for 10 min. Finally, the 0.5 M NaOH solution and 0.5 M L-ascorbic acid solution were prepared with deionized water to pour into beaker C and stirred for 120 min. After dropping to room temperature, the synthetic particles were obtained by centrifuging, washing and vacuum drying. The process is shown in Fig. 1(c).

2.3 Characterization

X-ray diffraction (Bruker, D8 Advance) and XRF (Bruker, S2 PUMA) of Cu Kα at a wavelength of 0.15406 nm were used to investigate the composition of the synthesized particles. TG tests were performed with the following parameters: 25 °C–800 °C, pure oxygen environment, and a temperature increase rate of 10 °C min^{-1}. The microstructure of copper particles was observed using field emission scanning electron microscopy (ZEISS, Gemini SEM 300). The sample preparation process was as follows: firstly, the obtained copper nanoparticles were ultrasonically dispersed in alcohol solution, then dropped onto the slides with a dropper and put into the oven for drying at 40 °C, and finally the sample was transferred to the specimen table. Fourier transform infrared spectrometer (Bruker, Tensor II) was used to measure the surface coating groups of copper particles.

3. Results and discussion

3.1 Synthesis of copper nanoparticle

The synthesis process of copper nanoparticles can be seen reflected in the changes of the solution color (Fig. 2). Fig. 2(a) shows the color change of the Step 1 and Step 2. The color change of Step 1 from the beginning to the end of the reaction (40 min) is green to white. With the interaction of blue copper complex ions and yellow copper tetrachloride complex ions, the color of solution turns to green.[22,23] The solution changes from green to white after 40 min means that Cu^{2+} has been reacted. After standing for a certain time, the solution has a white precipitation. It is speculated that the white precipitation is CuCl, since only CuCl crystal is white particle among all copper salts.[24] The color change of Step 2 from the beginning to the end of the reaction (60 min) was yellow-brown to red-brown, and further to dark-brown (blackish). When L-ascorbic acid and NaOH solutions were added, the solution color changed to yellow-brown, which indicated that the cuprous ions had started to be reduced to copper particles, and there were Cu^{1+} and Cu^{0} in the solution at this time. As the reaction proceeded, the number of Cu^{0} increased and the particle size was small. The color of the solution gradually changed from yellow-brown to red-brown and to dark-brown. It is presumed that the copper particles size is smaller than 100 nm due to the blackish solution color.

Fig. 2(b) shows the color change of the Step 3 from the beginning to the end of the reaction (160 min) in the order of green, white, light yellow, and red-brown. The solution appeared green at the beginning also due to the interaction of the blue copper complex ions and the yellow copper tetrachloride complex ions. After 40 min reaction, a white solution was produced. After a period of standing, there was a white precipitate, which is also speculated to be CuCl. The difference from the synthesis reactions of Step 1 and Step 2 is that the solution showed light yellow color after adding L-ascorbic acid and NaOH solutions. After standing for a certain time, there was a white precipitate in the solution, which indicates that there is still some CuCl particles that are not dissolved while Cu^{0} was prepared. As the reaction proceeded, due to the increase of Cu^{0}

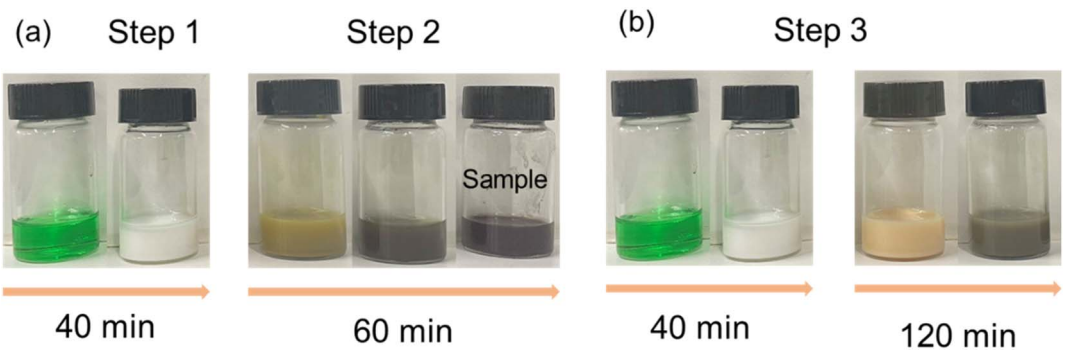

Fig. 2 Solution color change during copper nanoparticle synthesis of (a) Step 1 and Step 2; (b) Step 3.

and the slow dissolution of CuCl, the solution color turned to red-brown instead of dark-brown after 120 min. It is speculated that the large size copper particles were generated.

3.2 Characterization of copper nanoparticles

Fig. 3 shows the FESEM images of the synthesized particles. Fig. 3(a) shows the particles synthesized according to Step 1. The particles are mainly spherical as well as triangular, which is consistent with the reported shape of CuCl nanoparticles.[24,25] The CuCl nanoparticles are present as intermediates, and its metastable characteristics lead for the subsequent synthesis reaction. The synthesized intermediate CuCl nanoparticles have a particle size of about 25 nm and are well dispersed without agglomeration. Fig. 3(b) shows the final synthesis of copper nanoparticles according to Step 1 and Step 2. The intermediate CuCl particles from Fig. 3(a) were reduced to copper nanoparticles. The obtained nanoparticles are spherical, with a particle size of about 34 nm and good dispersion in solution without agglomeration and precipitation. After XRF analysis (Fig. 3(d)), it is shown that the synthesized nanoparticles were copper nanoparticles. Fig. 3(c) shows the particles synthesized according to Step 3. The obtained particles are irregular and the particle size increases to about 200 nm.

Fig. 4 shows the XRD, FTIR and TG curves of the synthesized particles. From Fig. 4(a), the XR diffractogram peaks at the values $2\theta = 28.5°$, 47.44°, 56.29° and 76.59°, corresponding to the CuCl structure synthesized by Step 1.[26] And it also conforms to the feature that the color of CuCl particles are white. The XR diffractogram peaks at the values $2\theta = 43.30°$ (Cu-111), 50.43° (Cu-200) and 74.13° (Cu-220),[27] corresponding to the Cu structure synthesized by Step 1 and Step 2. In addition to the characteristic peak of Cu, the XRD pattern contains a weak 2θ value of Cu_4O_3,[28] which indicates that a slight content of copper oxides are also present in the synthesized copper nanoparticles. It is speculated that the oxidation is because copper nanoparticles are extremely easy to be oxidized. From drying process to testing process in the experiment, copper nanoparticles are kept in the atmospheric environment, and a small amount of copper nanoparticles will inevitably be oxidized. The particles synthesized according to Step 3 also have 2θ values of copper as well as Cu_4O_3, but the intensity of peaks of copper is much lower than the intensity of copper nanoparticles synthesized according to Step 1 and Step 2, which implying a low crystallinity.

Therefore, we could conclude that the white intermediate nanoparticles synthesized in Step 1 are CuCl, and the nanoparticles synthesized by using the CuCl intermediate according to the synthesis method of Step 2 are copper nanoparticles with good crystallinity. The copper particles synthesized in Step 3 have low crystallinity and larger particle size, and the synthesis time and energy consumption are much higher than the copper nanoparticles synthesized by Step 1 and Step 2.

Fig. 4(b) shows the characteristic peak of pristine L-ascorbic acid (red curve) at 1753 cm^{-1} that represents the C=O stretching vibration, the characteristic peak at 1652 cm^{-1} that represents the C=C stretching vibration, and the characteristic peaks at 1314 cm^{-1} and 1023 cm^{-1} that represent the C–O–C asymmetric stretching vibration and the C–O–C symmetric stretching vibration, respectively. The characteristic peak at

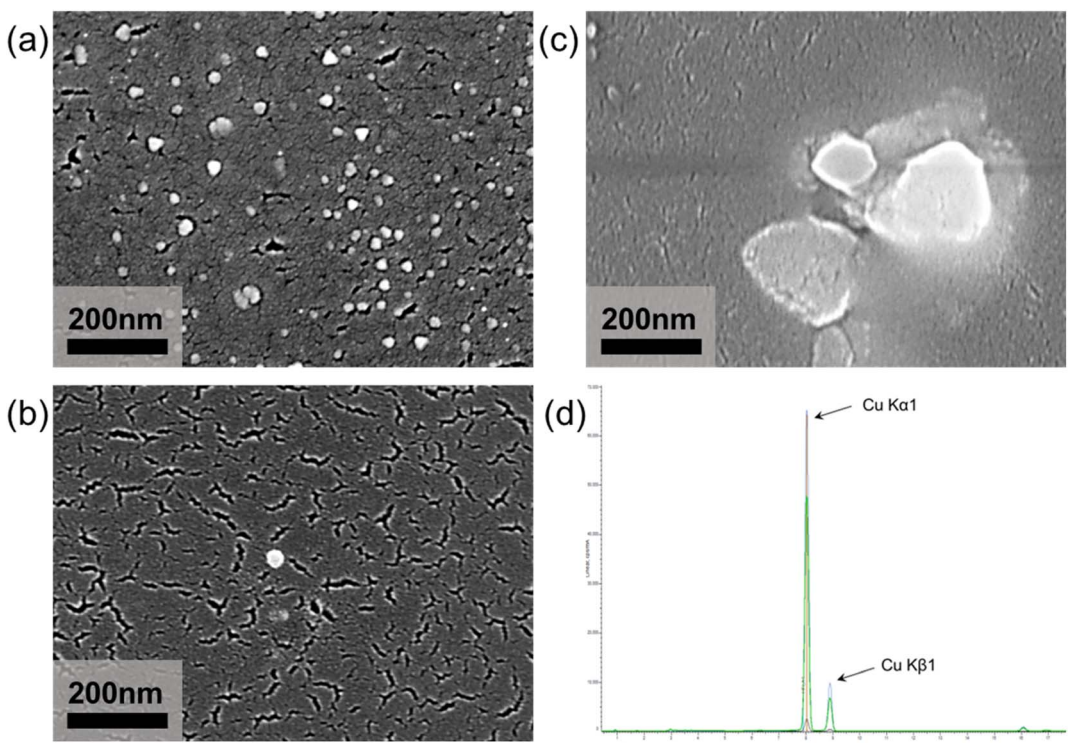

Fig. 3 FESEM images of (a) CuCl particles obtained by Step 1; (b) copper nanoparticle obtained by Step 1 and Step 2; (c) copper particles obtained by Step 3 and (d) XRF pattern of copper nanoparticle.

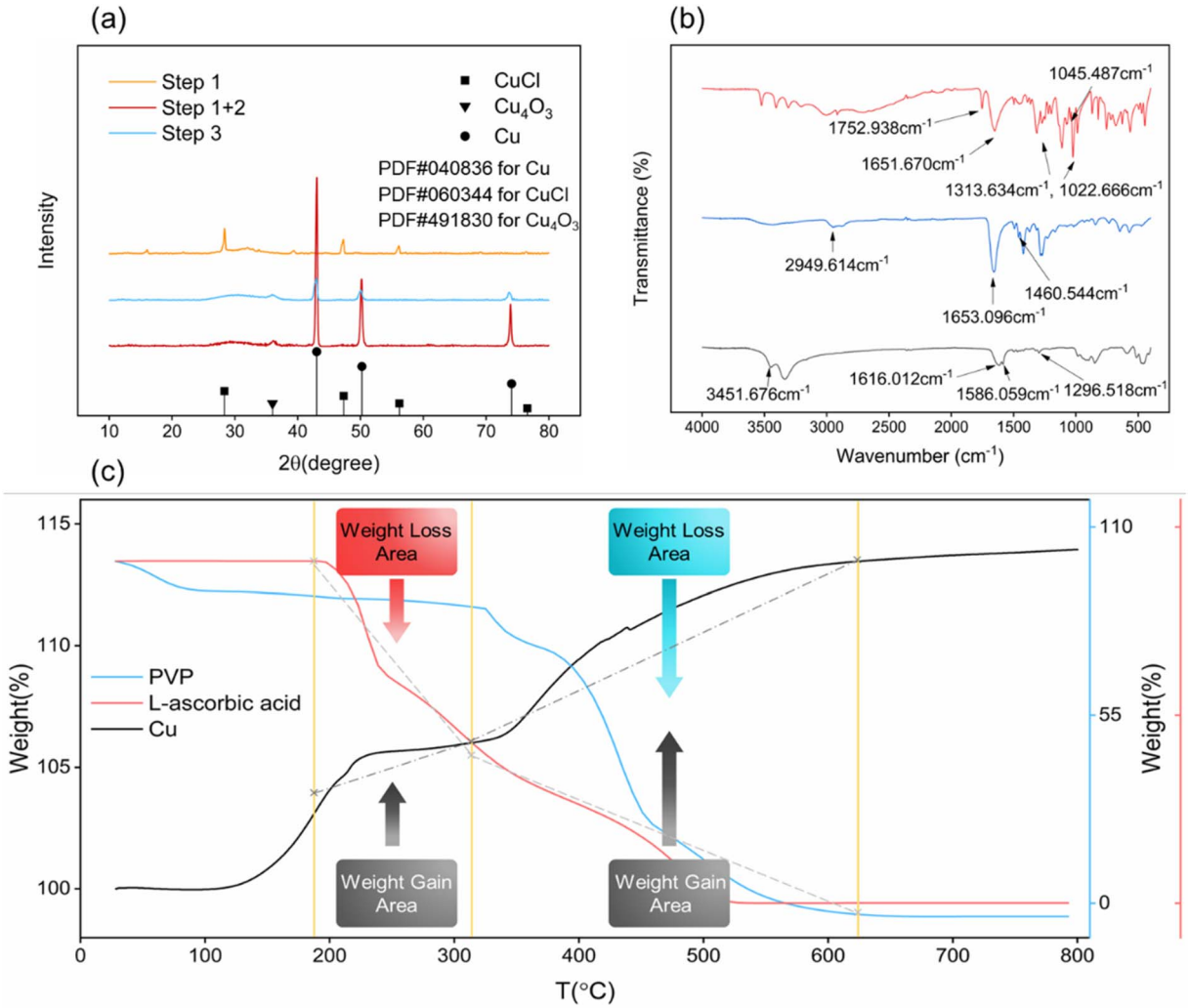

Fig. 4 (a) XRD pattern of synthesized copper nanoparticles obtained by Step 1 (yellow curve), obtained by Step 1 and 2 (red curve) and obtained by Step 3 (blue curve); (b) FTIR curve of pristine L-ascorbic (red curve), pristine PVP (blue curve) and synthesized copper nanoparticles (black curve); (c) TG curve of synthesized copper nanoparticles (black curve), pristine L-ascorbic acid (red curve) and pristine PVP (blue curve).

1045 cm^{-1} represents the –OH in-plane bending vibration. Moreover, the characteristic peak of the pristine PVP (blue curve) at 2950 cm^{-1} represents the asymmetric stretching vibration of CH_3^-, the characteristic peak at 1653 cm^{-1} represents the stretching vibration of the amide group, and the characteristic peak at 1461 cm^{-1} represents the asymmetric deformation vibration of CH_3^-. The characteristic peak of the synthesized copper nanoparticles (black curve) at 3452 cm^{-1} represents the N–H stretching vibration, and the characteristic peaks at 1616 cm^{-1}, 1586 cm^{-1}, 1297 cm^{-1} represent the C=O stretching vibration, the C=C stretching vibration and the C–O–C asymmetric stretching vibration, respectively. From the infrared spectra, the surface coating substance of the synthesized copper nanoparticles shows the N–H characteristic peaks instead of the amide characteristic peaks, and the C=O, C–O–C characteristic peaks, leading to the speculation that PVP and L-ascorbic acid reacted during the synthesis process, and this speculation could be confirmed from Fig. 4(c).

Fig. 4(c) shows the TG curves of the synthesized copper nanoparticles, pristine PVP and pristine L-ascorbic acid. There are two weight gain stages of copper nanoparticles. The first weight gain stage starts from near 150 °C to about 310 °C, and the second weight gain stage starts at 310 °C and ends at about 620 °C. We can see that the decomposition stages of L-ascorbic acid (red curve) and PVP (blue curve) correspond to the two weight gain stages of copper nanoparticles (black curve). At the first stage, when the pristine L-ascorbic acid starts to lose weight because of decomposition, the copper nanoparticles start to gain weight. As the temperature continues to increase, the pristine PVP starts to lose weight, at the same time the copper nanoparticles enter the second weight gain stage. Finally, as the decomposition of PVP ends, the copper nanoparticles are also completely oxidized and stop gaining weight. Therefore, we can demonstrate that during the synthesis process, the PVP and L-ascorbic acid reacted, resulting in the dehydrogenation product of L-ascorbic acid coating the surface of the copper

nanoparticles. In terms of weight gain in both stages (5 wt% in the first stage and 10 wt% in the second stage), the PVP is still the main coating material, and dehydrogenation product of L-ascorbic acid is the secondary coating material.

3.3 Effect of PVP molecular weight

Since many studies have shown that the molecular weight of PVP will affect the morphology of metal particles,[29] in this paper we also investigated the effect of PVP molecular weight on the morphology of copper nanoparticles. Fig. 5 shows the effect of different molecular weights of PVP on the morphology of copper particle. In order to give the crystals enough time to grow to obtain an easily recognizable crystal shape, the reaction time of Step 2 was uniformly adjusted to 180 min. It shows that when the molecular weight of PVP is 1 W, the synthesized copper particles are irregular shape as shown in Fig. 5(a). As the molecular weight of PVP increases to 4 W and 130 W, the synthesized copper particles are spherical and cubic as shown in Fig. 5(b) and (c), respectively. As the molecular weight of PVP increases, the shape of copper particles changes from irregular to spherical and finally the cubic.

This phenomenon is due to a great influence of the molecular weight of PVP on the morphology of copper particle. Under the conditions of different molecular weight or different reaction duration, the different crystal faces of copper particle will adsorb the PVP. The PVP will passivate the crystal face and inhibit the growth of the different crystal faces, implying a different growth rates of different crystal faces of copper particles during synthesis.[30,31] When the molecular weight of the PVP is low, the PVP will choose to combine with the {100} face, which has the lowest energy. The combined face will be passivated and stop growing. At this time, the {111} crystal face with higher energy will not be coated by the PVP. Thus, the {111} crystal face will not be passivated and could still grow freely, and the copper particles present as octahedron. Under the condition of high PVP molecular weight, the PVP has enough tendency to combine with {111} crystal face, the {111} crystal face will also be passivated. At this time, the {100} and {111} crystal faces are unable to grow freely, leading a cubic morphology.[32,33] When the molecular weight of PVP is in between, the morphology of copper particle will be transited from octahedron to cube, forming the spherical particles. As the conclusion, PVP molecular weight of 4 W was chosen to obtain spherical copper nanoparticles.

3.4 Effect of NaOH concentration

From the synthesis process, the solution turned from green to white in Step 1 by adding L-ascorbic, while the solution turned from green to yellow-brown instead of remaining white in Step 2 by adding L-ascorbic and NaOH. Thus, we need to figure out what role the NaOH plays in the color change of solution. The reducibility of L-ascorbic acid is reflected by an alkene glycol group contained on carbon 2 and carbon 3 of the five-membered ring. The entire metal reduction process is not a single step reduction, but a two-step reduction. First, L-ascorbic acid dissociates a hydrogen proton into semi-dehydroascorbic acid, and then the semi-dehydroascorbic acid dissociates another hydrogen proton into dehydroascorbic acid.[34] Therefore, one of the key factors for the reducibility of L-ascorbic acid is the pH value of the solution. With the dissociation of hydrogen protons, the pH value of solution will gradually decrease to acidic (hydrogen protons increase). At the same time, with the increase of hydrogen protons in the solution, the dissociation rate of hydrogen protons will slow down, leading to a weak reducibility. Thus, the addition of sodium hydroxide could effectively adjust the pH value of the solution and increase the reducibility of the L-ascorbic acid.

To determine the influence of NaOH concentration on reducibility, different NaOH concentrations are designed (see the details at Table 1). Fig. 6(a) shows the XRD patterns of the synthesized particles with different NaOH concentrations and Fig. 6(b) shows the color change images of the solution in Step 1 and Step 2. When only 0.5 M L-ascorbic acid was added, the synthesized particles are CuCl, which means that L-ascorbic acid reduces Cu^{2+} to Cu^{1+}. As the CuCl is white crystal and

Table 1 Formulation with different NaOH concentrations

Group	Cu^{2+} (M)	PVP (g)	L-Ascorbic acid (M)	NaOH (M)
1	0.37	0.25	0.5	0
2	0.37	0.25	0.5	0.25
3	0.37	0.25	0.5	0.5
4	0.37	0.25	0.5	0.75
5	0.37	0.25	0.5	1

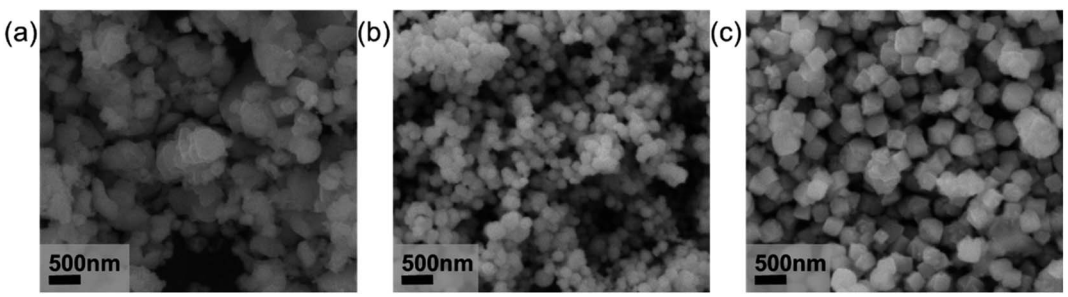

Fig. 5 SEM images of the synthesized copper particles with the PVP molecular weight of (a) 10 000; (b) 40 000 and (c) 1 300 000.

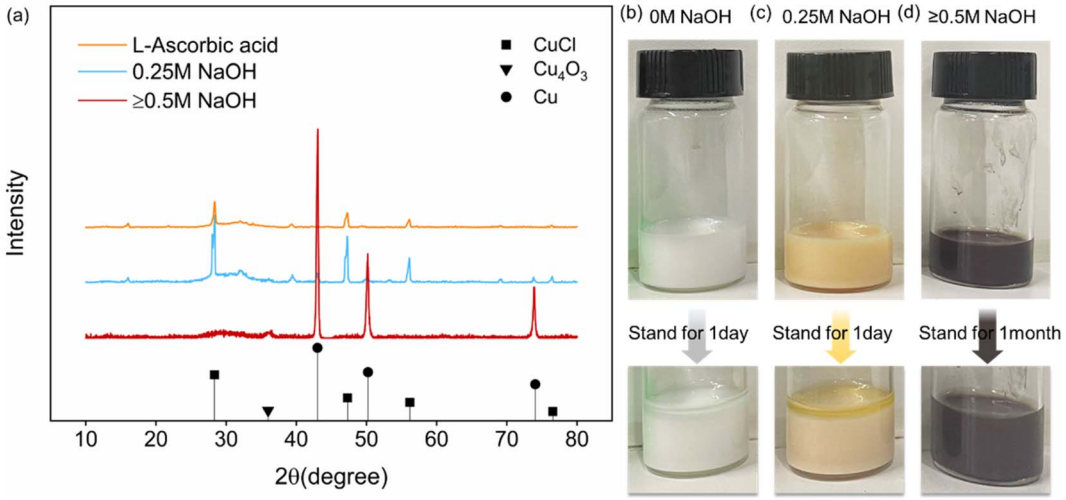

Fig. 6 (a) XRD pattern of synthesized copper nanoparticles with the NaOH concentrations of 0 M (yellow curve), 0.25 M (blue curve) and ≥0.5 M (red curve); (b) color change and dispersibility of the solutions with the NaOH concentrations of 0 M; (c) color change and dispersibility of the solutions with the NaOH concentrations of 0.25 M and (d) color change and dispersibility of the solutions with the NaOH concentrations of ≥0.5 M.

insoluble in ethylene glycol, we obtain the white solution. When 0.25 M NaOH and 0.5 M L-ascorbic acid solutions were added, the synthesized particles are primarily CuCl and a few copper particles with low crystallinity according to XRD pattern. The yellow-brown solution is obtained. When 0.5 M, 0.75 M, 1 M NaOH and 0.5 M L-ascorbic acid were added, the synthesized particles are copper nanoparticles. The dark-brown solution is obtained, and it remained good dispersion for 1 month without precipitation. The reason why the particles contain Cu_4O_3 is also because the copper nanoparticles are easy to be oxidized in the air.

It could be found that NaOH plays a major role in adjusting PH value during the synthesis process. The addition of NaOH facilitates the dissociation of hydrogen protons in L-ascorbic acid. When the concentration of NaOH is less than that of L-ascorbic acid, most of the L-ascorbic acid could only dissociate

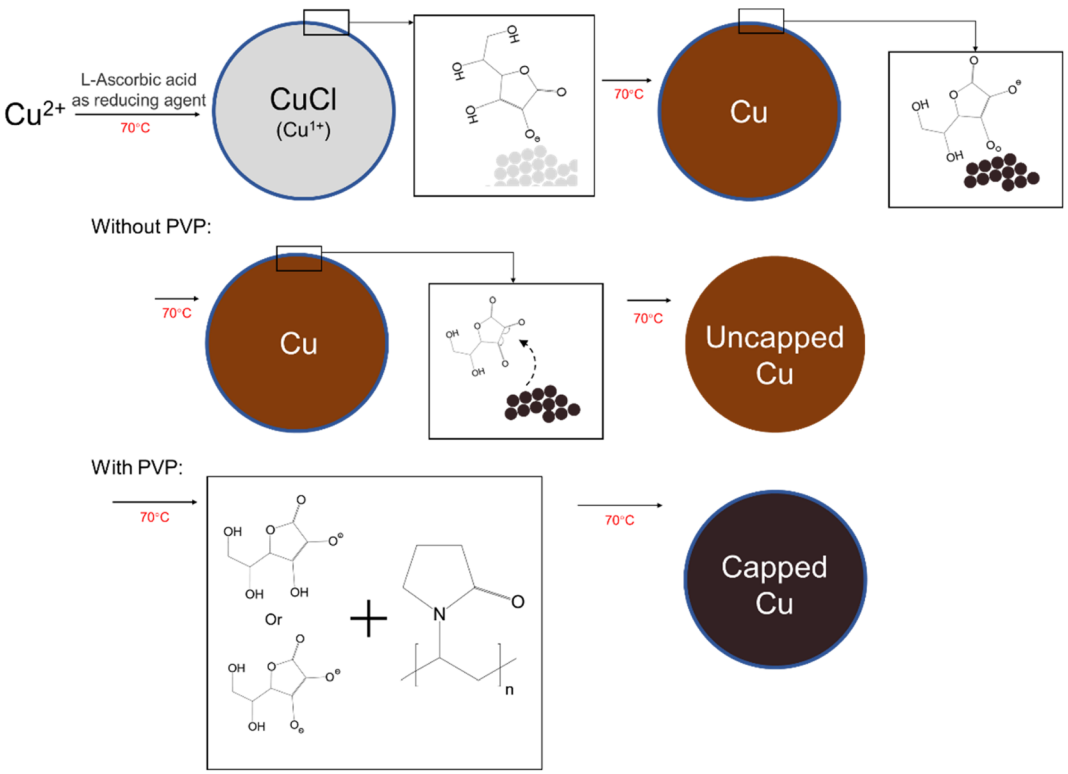

Fig. 7 Schematic diagram of reduction mechanism for the synthesized copper nanoparticles with and without PVP.

one hydrogen proton into semi-dehydroascorbic acid, reducing Cu^{2+} to Cu^{1+}. As the NaOH concentration increases, when the NaOH concentration is higher than the L-ascorbic acid concentration, L-ascorbic acid will dissociate two hydrogen protons into dehydroascorbic acid, reducing Cu^{2+} to Cu^{0}.

3.5 Reduction mechanism

From all the above analysis, it can be inferred that the possible mechanism of the synthesis in Step 1 and Step 2 should be divided into two steps. The first step is that L-ascorbic acid dissociates a hydrogen proton into semi-dehydroascorbic acid and reduces the Cu^{2+} to Cu^{1+}, forming CuCl intermediate. In solution, L-ascorbic acid will dissociate one hydrogen proton into semi-dehydroascorbic acid, which will reduce copper ions to cuprous ions. At this time, the further reduction of metastable CuCl is affected as the dissociation of hydrogen protons is hindered, then the cuprous ion cannot continue to be reduced to copper. Because of the short reaction time, the CuCl cannot grows further and remains a small size. Then, with addition of the NaOH solution and more L-ascorbic acid solution, sufficient hydrogen protons could be supplied to reduce the metastable CuCl, and the L-ascorbic acid is finally transformed from semi-dehydroascorbic acid to dehydroascorbic acid. The redox reaction is carried out smoothly and rapidly (as shown in Fig. 7), and the nano-sized copper particles are synthesized. The redox equation is shown as follows.

$$CuCl_2 \rightarrow Cu^{2+}$$

$$Cu^{2+} + C_6H_8O_6 \rightarrow CuCl + C_6H_7O_6^- + HCl$$

$$CuCl + C_6H_7O_6^- \rightarrow Cu^0 + C_6H_6O_6 + HCl$$

We added PVP for two important reasons. Firstly, PVP, as the main coating agent, can directly coat the surface of copper particles, which is beneficial to the dispersion and oxidation of copper particles. Secondly, and most importantly, PVP can react with L-ascorbic acid and its dehydrogenation products. Due to the formation of dehydroascorbic acid, it will automatically detach from the surface of copper nanoparticles, as shown in Fig. 7.[35] However, from the above analysis, it is clear that the L-ascorbic acid will react with the PVP, and the dehydrogenation product are partially coated on the surface of copper nanoparticles by supplemental coating where PVP fails to cover. Therefore, the copper nanoparticles are finally coated by the PVP and dehydrogenation product of L-ascorbic acid, which enhances the dispersibility and antioxidant properties of the copper nanoparticles.

4. Conclusion

In this study, we demonstrate a simple, fast and green method for the preparation of low-cost copper nanoparticles. By using L-ascorbic acid as the reducing agent and secondary capping agent, PVP as the primary capping agent, and NaOH as the pH modulator, the synthesized copper nanoparticles have a particle size of about 34 nm. The copper nanoparticles have good dispersion and no significant precipitation occurred even after 1 month of storage. By using a variety of analytical methods, we have demonstrated the possible reduction mechanism of using anhydrous copper chloride as the precursor to produce the intermediate cuprous chloride and finally synthesize copper nanoparticles. The reduction mechanism is a two-step reduction mechanism. At first, L-ascorbic acid dissociates a hydrogen proton into semi-dehydroascorbic acid, which reduces the copper ions to metastable intermediate CuCl. Due to the continued dissociation of hydrogen protons, CuCl is rapidly reduced to copper nanoparticles. With the addition of PVP, the reaction between L-ascorbic acid and PVP allows the dehydrogenation product of L-ascorbic acid to be coated on the surface of copper nanoparticles, which improves the dispersibility and antioxidation of the copper nanoparticles.

Since the non-toxic and green characteristics of the reaction, the synthesized copper nanoparticles could be used in medical and biological areas. In addition, the high stability of copper nanoparticles could be used as flexible conductive inks or flexible electronic paste material in the field of printing electronics.

Conflicts of interest

There are no conflicts to declare.

Acknowledgements

This work was supported by the Critical Research and Development Plan of Shaanxi Province, China (2020GXLH-Z-019, 2020GXLH-Z-009).

References

1 Q. M. Liu, Y. Takehiro, K. Kensuke and O. Masazumi, *Trans. Nonferrous Met. Soc. China*, 2012, **22**, 2198–2203.
2 S. R. Emory and S. Nie, *J. Phys. Chem. B*, 1998, **102**, 493–497.
3 M. A. El-Sayed, *Acc. Chem. Res.*, 2001, **34**, 257–264.
4 D. de Caro, M. Souque, C. Faulmann, Y. Coppel, L. Valade, J. Fraxedas, O. Vendier and F. Courtade, *Langmuir*, 2013, **29**, 8983–8988.
5 S. M. Harrell, J. R. McBride and S. J. Rosenthal, *Chem. Mater.*, 2013, **25**, 1199–1210.
6 A. Ghosale, R. Shankar, V. Ganesan and K. Shrivas, *Electrochim. Acta*, 2016, **209**, 511–520.
7 M. Dankoco, G. Tesfay, E. Benevent and M. Bendahan, *Mater. Sci. Eng.*, 2016, **205**, 1–5.
8 M. A. El-Sayed, *Acc. Chem. Res.*, 2001, **34**, 257–264.
9 K. S. Tan and K. Y. Cheong, *J. Nanopart. Res.*, 2013, **15**, 1–29.
10 R. Song, M. Yamaguchi, O. Nishimura and M. Suzuki, *Appl. Surf. Sci.*, 2007, **253**, 3093–3097.
11 S. D. Pike, E. R. White, A. Regoutz, N. Sammy, D. J. Payne, C. K. Williams and M. S. Shaffer, *ACS Nano*, 2017, **11**, 2714–2723.
12 Z. Liu and Y. Bando, *Adv. Mater.*, 2003, **15**, 303–305.
13 R. Y. Li and Y. S. Huang, *Dev. Appl. Mater.*, 2019, **3**, 70–76.

14 W. K. Han, J. W. Choi, G. H. Hwang, S. J. Hong, J. S. Lee and S. G. Kang, *Appl. Surf. Sci.*, 2006, **252**, 2832–2838.
15 N. Sarwar, S. H. Choi, G. Dastgeer, U. B. Humayoun, M. Kumar, A. Nawaz, D. I. Jeong, S. F. A. Zaidi and D. H. Yoon, *Appl. Surf. Sci.*, 2021, **542**, 148609.
16 W. Li, Q. Cen, W. Li, Z. Zhao, W. Yang, Y. Li, M. Chen, G. Yang and J. Yang, *J. Materiomics*, 2020, **6**, 300–307.
17 J. Valdez and I. Gomez, *J. Nanomater.*, 2016, **2016**, 9790345.
18 H. Sharghi, R. Khalifeh and M. M. Doroodmand, *Adv. Synth. Catal.*, 2009, **351**, 207–218.
19 N. Xia, Y. Cai, T. Jiang and J. Yao, *Carbohydr. Polym.*, 2011, **86**, 956–961.
20 N. Vigneshwaran, R. P. Nachane, R. H. Balasubramanya and P. V. Varadarajan, *Carbohydr. Res.*, 2006, **341**, 2012–2018.
21 R. S. Varma, *Green Chem.*, 2014, **16**, 2027–2041.
22 M. R. Bond, A. Gerdes and A. F. Kelley, *Acta Crystallogr.*, 2005, **61**, C301.
23 H. B. Yi, F. F. Xia, Q. B. Zhou and D. W. Zeng, *J. Phys. Chem. A*, 2011, **115**, 4416–4426.
24 Y. Huang, F. Shen, J. La, G. X. Luo, J. L. Lai, C. S. Liu and G. Chu, *Part. Sci. Technol.*, 2011, **31**, 81–84.
25 Z. H. Qiu, Q. F. Ruan, S. N. Huang, X. L. Huang, L. Song and Y. Yang, *J. Synth. Cryst.*, 2014, **43**, 2903–2907.
26 S. Mahtout, M. A. Belkhir and M. Samah, *Acta Phys. Pol., A*, 2004, **105**, 279–286.
27 C. Y. Chee and A. Azmi, *Int. J. Precis. Eng. Manuf.*, 2014, **15**, 1215–1221.
28 A. Zivkovic, J. Sheehama, M. E. A. Warwick, D. R. Jones, C. Mitchel, D. Likius, V. Uahengo, N. Y. Dzade, S. Meenakshisundaram and C. W. Dunnill, *Pure Appl. Chem.*, 2021, **93**, 1229–1244.
29 X. Huang and N. Zheng, *J. Am. Chem. Soc.*, 2009, **131**, 4602.
30 J. Yan, M. Q. Wang, S. G. Du, B. Wang and X. S. Zhang, *Ceram. Int.*, 2015, **41**, 3365–3371.
31 I. Washio, Y. J. Xiong, Y. D. Yin and Y. N. Xia, *Adv. Mater.*, 2006, **18**, 1745–1749.
32 K. M. Koczkur, S. Mourdikoudis, L. Polavarapu and S. E. Skrabalak, *Dalton Trans.*, 2015, **44**, 17883–17905.
33 X. Huang and N. Zheng, *J. Am. Chem. Soc.*, 2009, **131**, 4602.
34 J. Xiong, Y. Wang, Q. J. Xue and X. D. Wu, *Green Chem.*, 2011, **13**, 900–904.
35 Y. T. kwon, S. J. Yune, Y. Song, W. H. Yeo and Y. H. Choa, *ACS Appl. Electron. Mater.*, 2019, **1**, 2069–2075.